A lung targeted miR-29 mimic as a therapy for pulmonary fibrosis

Maurizio Chioccioli,[a] Subhadeep Roy,[b] Rachel Newell,[b] Linda Pestano,[b] Brent Dickinson,[b] Kevin Rigby,[b] Jose Herazo-Maya,[c] Gisli Jenkins,[d] Steward Ian,[d] Gauri Saini,[f] Simon R. Johnson,[f] Rebecca Braybrooke,[f] Guying Yu,[e] Maor Sauler,[a] Farida Ahangari,[a] Shuizi Ding,[h] Joseph Deluliis,[a] Nachelle Aurelien,[g] Rusty L. Montgomery,[b]* and Naftali Kaminski[a]*

[a]Pulmonary, Critical Care and Sleep Medicine, Yale School of Medicine, New Haven, CT, USA
[b]miRagen Therapeutics, Inc, Boulder, CO, USA
[c]University of South Florida, Tampa, FL, USA
[d]National Heart and Lung Institute, Imperial College London, London, UK
[e]State Key Laboratory of Cell Differentiation and Regulation, College of Life Science, Henan Normal University, Xinxiang, CN, China
[f]University of Nottingham, Nottingham UK
[g]Hospital Medicine, Weill Cornell School of Medicine, NY, NY, USA
[h]Department of Pulmonary and Critical Care Medicine, The Second Xiangya Hospital of Central South University, Changsha, Hunan, China

eBioMedicine 2022;85: 104304
Published online xxx
https://doi.org/10.1016/j.ebiom.2022.104304

Summary

Background MicroRNAs are non-coding RNAs that negatively regulate gene networks. Previously, we reported that systemically delivered miR-29 mimic MRG-201 reduced fibrosis in animal models, supporting the consideration of miR-29-based therapies for idiopathic pulmonary fibrosis (IPF).

Methods We generated MRG-229, a next-generation miR-29 mimic based on MRG-201 with improved chemical stability due to additional sugar modifications and conjugation with the internalization moiety BiPPB (PDGFbetaR-specific bicyclic peptide)[1]. We investigated the anti-fibrotic efficacy of MRG-229 on TGF-β1 treated human lung fibroblasts (NHLFs), human precision cut lung slices (hPCLS), and in vivo bleomycin studies; toxicology was assessed in two animal models, rats, and non-human primates. Finally, we examined miR-29b levels in a cohort of 46 and 213 patients with IPF diagnosis recruited from Yale and Nottingham Universities (Profile Cohort), respectively.

Findings The peptide-conjugated MRG-229 mimic decreased expression of pro-fibrotic genes and reduced collagen production in each model. In bleomycin-treated mice, the peptide-conjugated MRG-229 mimic downregulated profibrotic gene programs at doses more than ten-fold lower than the original compound. In rats and non-human primates, the peptide-conjugated MRG-229 mimic was well tolerated at clinically relevant doses with no adverse findings observed. In human peripheral blood from IPF patients decreased miR-29 concentrations were associated with increased mortality in two cohorts potentially identified as a target population for treatment.

Interpretation Collectively, our results provide support for the development of the peptide-conjugated MRG-229 mimic as a potential therapy in humans with IPF.

Funding This work was supported by NIH NHLBI grants UH3HL123886, R01HL127349, R01HL141852, U01HL145567.

Keywords: Idiopathic pulmonary fibrosis; MicroRNA; miR-29; RNA therapies

*Corresponding authors.
E-mail addresses: rusty.montgomery@gmail.com (R.L. Montgomery), naftali.kaminski@yale.edu (N. Kaminski).

Research in context

Evidence before this study

In the search for modifiers of complex disease phenotypes, oligonucleotide (ON) technologies, with their rich array of modalities and capabilities for gene silencing, gene activation and splice modulation, are of particular interest.[1] Progress towards their clinical translation into approved, effective and safe therapies continues to be made.[2–4] Within ON therapies, microRNAs have been shown to regulate normal lung development, maintenance of different lung cell populations, and participate in the lung's response to injury and repair and their levels are changed in advanced lung disease, including Idiopathic Pulmonary Fibrosis.[5–10] Among microRNAs, the miR-29 family has been extensively studied as a potential anti-fibrotic regulator based on its regulation of direct and downstream targets Collagen I and III, IGF1, and CTGF.[11,12] Although constitutively highly expressed, its expression levels are decreased in kidney,[13] lung,[14,15] liver, and myocardial fibrosis,[16] suggesting that supplementing miR-29 could be a therapeutic strategy for reversing or mitigating organ fibrosis. In earlier work, we demonstrated that a first-generation synthetic ON mimic of miR-29b; Remlarsen/MRG-201, blunted fibrosis in the bleomycin-induced pulmonary fibrosis mouse model.[15] In addition, in a randomized phase 1 clinical trial, intradermally administered Remlarsen/MRG-201 reduced collagen expression and delayed onset of fibroplasia in healthy volunteers, consistent with a broad anti-fibrotic therapeutic mechanism.[17] However, microRNA mimics are unstable compounds and present numerous challenges for clinical translation.[18] Due to their size and charge, oligonucleotide-based compounds cannot passively enter cells, and are vulnerable to nuclease degradation,[19] sequestration in non-target tissues, and endo-lysosomal misrouting and degradation.[1] These vulnerabilities can be mitigated with backbone modifications (replacing one of the non-bridging oxygens of inter-nucleotide phosphate groups with sulphur atoms to create phosphorothioate (PS) linkages) that retard nuclease degradation as well as increases circulation duration as clearance via the kidneys is reduced.[20] In addition, 2′-O-methy or 2′-Fluoro- ribose sugar modifications further limit nuclease degradation and increase plasma stability. Finally, therapeutic ON delivery can be increased and directed through covalent conjugation with bioactive molecules such as lipids, cholesterol or tissue-targeting agents such as peptides.[21]

Added value of this study

We generated MRG-229, a next-gen miR-29 mimic with improved stability and potential for targeted delivery. In cultured human lung fibroblasts and lung slice cultures, we demonstrate that MRG-229 can reduce TGF-β induced fibrosis, as evidenced by downregulation of direct and downstream miR-29 targets COL1A1 and ACTA2, respectively, at a 10-fold lower concentration than MRG-201. Similarly, in the bleomycin-induced mouse fibrosis model, we find that MRG-229 treatment counteracted upregulation of fibrosis-associated gene programs. At therapeutic dosing levels, MRG-229 therapy is associated with a favourable safety profile in mice, rats, and non-human primates (NHPs). Finally, decreased concentrations of circulating miR-29 in the peripheral blood of patients with IPF are associated with substantially reduced survival.

Implications of all the available evidence

These findings suggest that MRG-229 is an attractive preclinical candidate for therapeutic development in fibrosis-associated lung indications and potentially other fibrotic conditions.

Introduction

MicroRNAs have been shown to regulate normal lung development, maintain different lung cell populations, and participate in the lung's response to injury and repair; and their levels are changed in advanced lung disease, including Idiopathic Pulmonary Fibrosis,[5–10] a progressive, invariably lethal lung disease with two FDA approved therapies, which only slow down disease progression.[22,23] Among microRNAs, the miR-29 family has been extensively studied as a potential anti-fibrotic regulator based on its regulation of direct and downstream targets Collagen I and III, IGF1, and CTGF.[11,12] Although constitutively highly expressed, its expression levels are decreased in kidney,[13] liver,[24] myocardial fibrosis[16] and pulmonary fibrosis,[14,15] suggesting that supplementing miR-29 could be a therapeutic strategy for reversing or mitigating organ fibrosis. In earlier work, we demonstrated that a first-generation synthetic oligonucleotide mimic of miR-29b; Remlarsen/MRG-201 (hereafter referred to as MRG-201), blunted fibrosis in the bleomycin-induced pulmonary fibrosis mouse model.[15] In addition, in a randomized phase 1 clinical trial, intradermally administered MRG-201 reduced collagen expression and delayed onset of fibroplasia in healthy volunteers, consistent with a broad anti-fibrotic therapeutic mechanism.[17]

These observations supported the consideration of miR-29 based therapies for IPF. Here we describe MRG-229, a miR-29 mimic with improved chemical stability and conjugated to an internalization moiety BiPPB (bicyclic platelet-derived growth factor beta receptor PDGFβR-binding peptide), that demonstrated substantial antifibrotic activity *in-vitro*, *ex-vivo*, and *in-vivo*. In cultured NHLFs and hPCLS, MRG-229 reduces TGF-β1-induced increases in COL1A1 and ACTA2. Similarly, in the bleomycin-induced mouse fibrosis model, intravenous or subcutaneous MRG-229 blunted fibrosis equally regardless if used in preventative or therapeutic experimental designs. Assessment of safety demonstrated that MRG-229 was not associated with adverse effects in mice, rats, or non-human primates (NHPs).

Finally, decreased concentrations of circulating miR-29 in the peripheral blood of patients with IPF are associated with substantially reduced survival. Taken together, these findings suggest that MRG-229 is an attractive preclinical candidate for therapeutic development in fibrosis-associated lung indications and potentially other fibrotic conditions.

Methods

Animals

All animal studies were conducted in accordance with the NIH guidelines for humane treatment of animals and were approved by the Animal Care and Use Committee (IACUC Animal Protocol # 2017-11592) at MiRagen Therapeutics, Inc. and at Yale University.

Cell culture

Normal Human Lung Fibroblasts (NHLFs) (LONZA Cat. # CC-2512), were cultured in Fibroblast Growth Medium (FGM) (LONZA Cat. # CC-3132) supplemented with Fibroblast Growth Factor (FGF, LONZA Cat. # CC-4068) and maintained at 37°C and 5% CO_2. LL 29 (ATCC CCL-134™) cells were maintained in Ham's F12K medium (ThermoFisher Cat. # 11765047) with 15% FBS (ThermoFisher Cat. # 10082147) and maintained at 37°C and 5% CO_2. Proliferation and viability were assessed using the WST-1 assay (Sigma Cat. # 5015944001).

Oligonucleotide synthesis

In vitro and *in vivo* studies utilized oligonucleotides that were produced via solid phase support synthesis at miRagen and formulated in PBS. All oligonucleotides were sterile filtered during formulation. Vehicle control for animal studies was sterile PBS.

Quantitative real-time PCR analysis. To quantify *in vitro* regulation of pro-fibrotic genes *COL1A1* and *ACTA2*, NHLFs were treated with 5ng/mL TGF-b (Cat. # 240-B-002/CF, R&D Systems) to induce the fibrotic response. Cells were then treated with MRG-229 through passive administration at concentrations ranging from 0.3 to 10 mM or through transfection at concentrations ranging from 5nM to 50nM at 0.2 mL/well Dharmafect I (Horizon Cat. # T-2001-02) as per the manufacturer's instructions. After 72h, samples were harvested, and mRNA expression levels analysed with RT-qPCR (Life Technologies) using human Col1a1 and Acta2 primers from ABI (Applied Biosystems) for the specified gene and species.

For *in vivo* real-time PCR analysis, 50-100 mg of tissue was homogenized in 1 mL Trizol (ThermoFisher Cat. # 15596026) in Lysing Matrix D tubes (MP Biomedicals Cat. # 116913050-CF) with shaking for 4 × 20 seconds using an Omni BeadRuptor 24 (Omni Intl.) at a speed of 5.65. Total RNA was extracted as per the manufacturer's standard protocol, after which 5 μL of 125 ng/μL RNA from each tissue sample was used to generate cDNA using Applied Biosystems High-Capacity cDNA Reverse Transcription Kit (ThermoFisher Cat. #18090010) per manufacturer's specifications. The expression of a subset of genes was analysed by quantitative real time PCR using Taqman probes (Applied Biosystems).

Hydroxyproline assay in cultured cells

Samples of untreated and TGF-b treated LL 29 supernatant, and samples that had also received increasing concentrations of MRG-229, were dried until constant weight and hydrolysed in 12 N HCl (Sigma Cat. # 1090601003) overnight at 120°C and then dried by evaporation for 3 h at 120°C. Hydroxyproline was then detected using an in-house LC MS/MS assay developed at MiRagen. Data are expressed as percent difference relative to untreated LL 29 cells.

Procollagen IC-peptide (PIP) analysis

PIP secretion in NHLFs treated with MRG-201 or MRG-229 was assessed by testing the supernatant of treated cells in a procollagen type I PIP ELISA (Takara Cat. # MK101).

Prophylactic paradigm

Bleomycin-treated mice were dosed through intravenous injection with saline, MRG-201 100 mpk (mg/Kg) on days 3, 7, 10 and 13. On day 14, animals were sacrificed, and lung tissue analysed for % total lung collagen quantified by Orbit machine learning image analysis software, qPCR analysis of downregulated gene expression levels of a panel of fibrosis-associated genes.

Therapeutic dosing

Bleomycin-treated mice were dosed through intravenous injection with saline, MRG-201 at 100 mpk, or MRG-229 at 10 mpk, on days 10, 13, 17 and 20. On day 21, animals were sacrificed, and lung tissue IGF-1 levels in bronchoalveolar lavage fluid and TIMP-1 levels in serum were analysed by ELISA. Mean % total lung collagen quantified by Orbit machine learning image analysis software.

Human precision cut lung slice (hPCLS) culture

Human lung segments were obtained through the National Disease Research Interchange (NDRI Protocol ID: RKAN1 01 002C)) and hPCLS generated as previously described.[25] Briefly, low melting-grade agarose (3 wt-%) (Sigma Cat. # A9045) was slowly injected via a visible bronchus to artificially inflate the lung segments. Segments were cooled at 4°C for 30 minutes to allow gelling of the agarose and then cut to a thickness of 300µm using a Compresstome (VF-300-0Z by

Precisionary) at cutting speed of 6 μm s^{-1} and oscillation frequency of 5Hz. The hPCLS were cultured in 24 multiwell plates in 500μL DMEM-F12 no-phenol red (Gibco Cat. # 21041025) containing 0.1% FBS (ThermoFisher Cat. # 10082147) and 1% Streptomycin, Amphotericin B, Penicillin 100X (Gibco Cat. # 15240096).

Fibrosis model in hPCLS cultures

hPCLS, 3 slices for each experimental condition, were exposed to a fibrosis-inducing media (transforming growth factor-β (TGF-β) (Cat. #240-B-002/CF, R&D Systems), 5 μM platelet-derived growth factor-AB (PDGF-AB) (Cat. # PHG0134, GIBCO), 10 ng/ml tumor necrosis factor-α (TNF-α) (Cat. # P06804, R&D Systems), and 5 μM lysophosphatidic acid (LPA) (Cat. # 62215, Cayman Chemical) or a control cocktail (including vehicle control) for 120h with media replaced every 24h as previously described.[25] In this blinded experiment, fibrosis-induced slices were treated with MRG-229 (sample #2), a cholesterol-conjugated miR-29 mimic (sample #4), each at 200μM final concentration, or control (samples #1, #3). After 5 days after treatment, lung slices were processed for analysis; divided for histology and RT-qPCR analysis, respectively.

Histology on hPCLS

hPCLS were fixed with 4% paraformaldehyde (ThermoFisher Cat. # FB002) overnight, and paraffin-embedded at 0h and 120h. 3μm sections were cut using a microtome, mounted on glass slides, and subjected to antigen retrieval. After deparaffinization and rehydration, staining was performed according to standard protocols for Masson's Trichrome, and samples mounted using mounting medium (VectorLabs Cat. # H-5700-60) and covered with a cover slip. For collagen quantification, bright field scanning with a Nikon inverted microscope at 20X magnification was used to acquire two representative images for each sample and at least 20 different random field of views as previously described.[26] Collagen staining was quantified and determined by percentage of stained areas. Images were analysed with ImageJ software (ImageJ NIH).

Histology

Samples were sent to HistoTox Labs (Boulder CO USA) for paraffin embedding, sectioning, and staining with Hematoxylin and Eosin and Masson's Trichrome. Masson's Trichrome sections were evaluated for collagen deposition and fibrotic mass using Orbit image analysis (Orbit Idorsia Pharmaceuticals Ltd). Full sections were evaluated for the % collagen in the whole tissue, for the % collagen in the lung tissue and fibrotic mass (excluding structural collagen), for the % collagen in the lung tissue (excluding structural collagen and fibrotic mass), and for the % tissue area that was fibrotic mass (excluding structural collagen and normal lung tissue).

Biodistribution analysis

A sandwich hybridization assay was used for the quantification of promiR-29 in tissue samples. Probes for the hybridization assay were synthesized using 2'Ome, and LNA modified nucleotides (TriLink Biotech). Detection was accomplished using anti-fluorescence-POD, Fab fragments (Sigma Cat. # 11426346910) and TMB Peroxidase Substrate (KPL) (Seracare Cat. # 5120-0047 50-76-00). Standard curves were generated using non-linear logistic regression analysis with 4 parameters (4-PL). The working concentration range of the assay was 2-2000 ng/mL. Tissue samples were prepared at 100 mg/mL by homogenizing in 3M GITC buffer (3 M guanidine isothiocyanate, 0.5 M NaCl, 0.1 M Tris pH 7.5, 10 mM EDTA) for 2 × 45 seconds using an Omni BeadRuptor 24 (Omni Intl.) at a speed of 5.65. Tissue homogenates were diluted a minimum of 50-fold in 1 M GITC Buffer (1 M guanidine isothiocyanate, 0.5 M NaCl, 0.1 M Tris pH 7.5, 10 mM EDTA) for testing.

RNA isolation and RT-qPCR on PCLS

hPCLS samples were snap frozen in liquid nitrogen and homogenized using a hand-held homogenizer (Bio-Gen Cat. # 01-01200). QIAGEN miRNA was used for total RNA isolation (QIAGEN Cat. # 217684). The RNA concentration and quality were assessed using NanoDrop spectrophotometer. Relative expression of MiR-29 targets genes *COL1A1* and *COL3A1* mRNA levels from all *ex-vivo* experiments were determined by RT-qPCR using TaqMan gene expression assays (Applied Biosystems). Reverse transcription with random primers and subsequent PCR were performed with TaqMan RNA-to-CT 1-Step Kit (ThermoFisher Cat. # 4392653). All experimental groups were assessed as 6 technical replicates and repeated at least three times. Raw data for cycle threshold (Ct) values were calculated using the ViiA7 v.1 software (Applied Biosystems) with automatically set baseline. The results were analysed by the ΔΔCt method and normalized to GAPDH. Fold change was calculated by taking the average over all the control samples as the baseline. All the probes used in this study were purchased from Thermo Fisher Scientific.

Bleomycin model of pulmonary fibrosis

Male C57Bl/6 mice, 9-10 weeks of age, were purchased from Taconic Biosciences, Hudson, NY and allowed to acclimate for at least one week prior to experiments. Mice were anesthetized with dexmedetomidine (Sigma Cat. # SML0956), 1 mg/kg IP, intubated, and given one, intra-tracheal dose of bleomycin (McKesson Corporation Cat. # 1129996) at 1.25 mg/kg in 50uL saline or an equivalent volume of saline. A reversal agent was given subcutaneously once the mice had been dosed.

Animals were then treated with MRG-201, MRG-229, or an equivalent volume of 0.9% saline by intravenous injection and euthanized on days 8, 14, and 21 after bleomycin administration. Serum and BALF samples were collected as well as tissue samples. Serum was collected and used for measurement of ALT (Sigma Cat. # MAK052), AST (Sigma Cat. # MAK055), BUN (Sigma Cat. # MAS008), and creatinine activity (Sigma Cat. # MAK080). Bronchoalveolar lavage fluid (BALF) was collected, spun at 1200 x g for 15 min after which supernatant and pellet were separated and frozen. BALF supernatant will be decanted/collected and placed in a separate 1.5 mL Eppendorf tube. BAL cell pellets and supernatant will then be frozen and stored. The left lobe of the lung was dissected and used for histology and molecular assessment, whereas the right caudal lobe was flash frozen in liquid nitrogen and used for hydroxyproline/collagen assays and biodistribution analysis. Liver, kidney, spleen, and heart tissue was also collected and flash frozen.

Exosomal miRNA isolation from IPF cohorts

Participants. 46 and 213 patients with IPF diagnosis were recruited from Yale and Nottingham Universities, respectively. IPF diagnosis was based on guidelines of the American Thoracic Society and European Respiratory Society.[22] Patients were followed until death or loss of follow up. Follow up time was limited to three years.

Sample collection, Yale University cohort: Blood was collected in heparin tubes using a routine procedure and was immediately (within 10 minutes after blood collection) centrifuged at 4°C, 1200 × g, for 10 min). Plasma was aliquoted and frozen at −80°C until analysis. All patients provided written informed consent and a protocol incorporating biomarker-studies was approved by the Institutional Review Board (IRB), Yale School of Medicine (HIC#0706002766).

Sample collection, Profile cohort. Exosomal miRNA isolation: Briefly, 400µl plasma or serum were used as starting material for exosomal miRNA's extraction using Plasma/Serum Circulating and Exosomal RNA Purification Mini Kit (Norgen Biotek Cat. # Dx42800). To detect circulating and exosomal miR-29b levels, we used multiplexed, color-coded probe pairs (Nanostring nCounter analysis system) using 20 ng of total RNA, following the manufacturer's protocol. All patients provided written informed consent and a protocol was approved by Central England Ethics Approval Number (IRB) REC ref. 10/H0402/2)

Statistical analysis

miRNA data was normalized using top 100 normalization and log2 transformed miR-29b levels were used for statistical analysis. Receiver Operating characteristics (ROC) curves were used to determine the optimal threshold for mortality prediction using exosomal miR-29b in IPF patients from both Yale and Profile cohorts. Cox proportional hazard's models and Kaplan-Meier curves were used to determine the association between exosomal miR-29b levels, adjusted to GAP index, and IPF mortality. We compared the resulting metabolic activities of the treatment groups and controls using one-way analysis of variance (ANOVA) and Tukey's multiple-comparison post-test. Differences between groups were significant at a P value of <0.05. Statistical analyses were performed with GraphPad Prism 5.0 (GraphPad Software, Inc., San Diego, CA).

Role of funders

Funders had no role in study design, data collection, data analysis, interpretation, or writing of report.

Results

Design of the next-geneneration miR-29 mimic

MiRNA mimics are chemically synthesized double-stranded RNA molecules designed to elicit biologic activity by imitating mature miRNA duplexes. To achieve therapeutic efficacy, mimics must be stabilized to ensure a long half-live after administration.[1] To identify next-generation miR-29 mimics with improved *in vivo* stability, we performed an iterative discovery chemistry screen starting with MRG-201, our first-generation double strand miR-29 mimic.[15] Our aim was to minimize nuclease-mediated degradation while maintaining RNA-induced silencing complex (RISC) loading and activity. In the resulting miR-29 mimic, all unmodified RNA residues were replaced with either a 2'F or 2'O-Me modified ribose sugars. Next, we assessed whether conjugation of BiPPB, known to target cargo to pro-fibrotic cells for internalization,[27] could improve targeted delivery. After having optimized the stabilization modifications, we conjugated BiPPB to our modified miR-29 mimic, which we named MRG-229 (Figure 1). We also conjugated the miR-29-mimic to a cholesterol moiety to compare it to MRG-229 in downstream experiments.

MRG-229 reduces fibrosis-associated phenotypes in NHLFs and hPCLS

To confirm that the added modifications did not interfere with miRNA mimicking activity, we assessed MRG-229 in NHLFs treated with TGFβ to induce pro-fibrotic genes. In control TGFβ-treated NHLFs, we found robustly increased expression of *COL1A1* (a direct miR-29 target) and *ACTA2* (a downstream effector of fibrotic signalling). In contrast, in the presence of MRG-229, *COL1A1* and *ACTA2* gene expression levels were reduced in a dose-dependent manner (Figure 2a, b). These data demonstrate that MRG-229 retains the

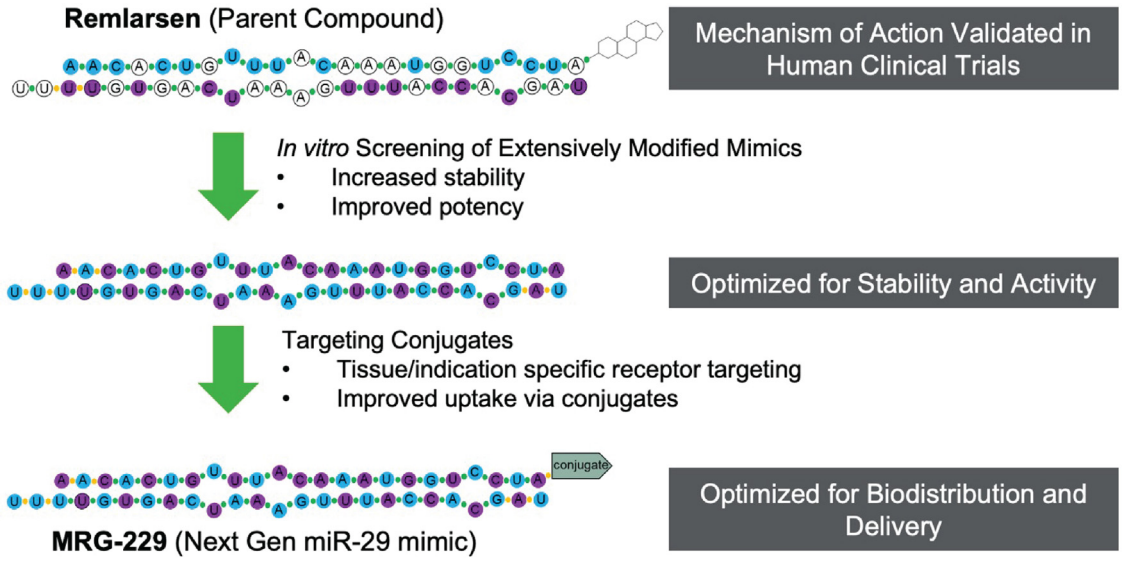

Figure 1. Overview of modifications differentiating second-geneneration miR-29 from first gen MRG-201/Remlarsen. Top, first-gen MRG-201, the parent compound, bottom, MRG-229 (Next generation miR-29 mimic), the second-gen compound. DNA bases: white circles = unmodified base, blue circles = 2'OMe, purple circles = 2'F, linkages: green circles = phosphorodiester linkage, orange circles = phosphorothioate (PS) linkage. NH2 terminus modification: MRG-201/Remlarsen = cholesterol, BiPPB = platelet-derived growth factor beta receptor (PDGFβR)-binding peptide (BiPPB).

anti-fibrotic properties of MRG-201 through regulating the expression of miR-29 direct and downstream targets (Figure 2a-b). We next compared the MRG-229-induced anti-fibrotic gene effects to MRG-201 by assessing Pro-collagen I C-peptide (PIP), a marker of newly synthesized, secreted collagen, without impacting cell viability. To this end, we administered MRG-229 or MRG-201 to TGFβ-treated NHLFs at concentrations ranging from 0.3-10 μM, assessed for cell viability using the WST-1 mitochondrial dehydrogenase assay, and PIP levels in cell culture supernatant by ELISA. Cell viability in MRG-229-treated NHLFs was significantly improved relative to MRG-201-treated NHLFs, indicative of a higher tolerance of MRG-229. Although even low doses of MRG-201 reduced cell viability, with the highest 10 μM dose being toxic (25% viability), only the highest dose of MRG-229 (10 μM) reduced viability (75% viability) with the second highest dose (5 μM) being equivalent to control (Figure 2c). We also observed MRG-229 robustly inhibited PIP, and at a superior potency relative to MRG-201 (Figure 2d).

To assess whether similar effects could be achieved in already diseased cells, we treated LL29 fibroblasts (a cell line derived from a young female patient with pulmonary fibrosis) with TGFβ followed by increasing concentrations of MRG-229. After 72 hours, we assessed collagen synthesis and secretion by assessing hydroxyproline levels by liquid chromatography-mass spectrometry. Relative to TGFβ treatment alone, MRG-229 significantly reduced cumulative hydroxyproline levels by 0.9 at 0.1μM, 1.1 at 0.5μM, 1.2 at 1 and 3μM (Figure 2e). Together, these data demonstrate that MRG-229, with a greater potency and tolerability than MRG-201, mitigates TGFβ-induced upregulation of fibrosis-associated genes and blunts collagen synthesis and secretion in normal and IPF cells *in vitro*.

Next, we assessed how MRG-229 regulates collagen production in hPCLS as previously described.[25,28,29] Briefly, 300μm thick hPCLS derived from donors without a history of lung disease, were treated with control medium or medium containing a profibrotic cocktail (FC) (5 μg TGFβ, 50 μg PDGF-AB, 10 ng TNFα, and 10 mg LPA) for 5 days, after which we assessed expression of *COL1A1*, *COL3A1* (Figure 3a, b), and collagen levels (Figure 3d, e). MRG-229-treated hPCLS had reduced expression of *COL1A1* and *COL3A1* (Figure 3a, b), and collagen levels (Figure 3d, e). In both experiments, MRG-229 activity was comparable to the activity of the miR-29-mimic with a conjugated cholesterol moiety. A BiPPB-conjugate or cholesterol conjugate to the non-targeting control oligonucleotide had no effect (Figure 3a, b). These data confirm that MRG-229 reduces experimentally induced fibrotic activity in both *in vitro* and *ex vivo* human disease models. Last, we assessed miR-29 levels in hPCLS exposed to FC (Figure 3c). PCR confirmed reduction of miR-29 levels after 120h of exposure to FC comparing to non-treated.

MRG-229 shows robust anti-fibrotic activity *in vivo*

To assess *in vivo* activity of MRG-229, we used two dosing paradigms in the bleomycin-induced pulmonary

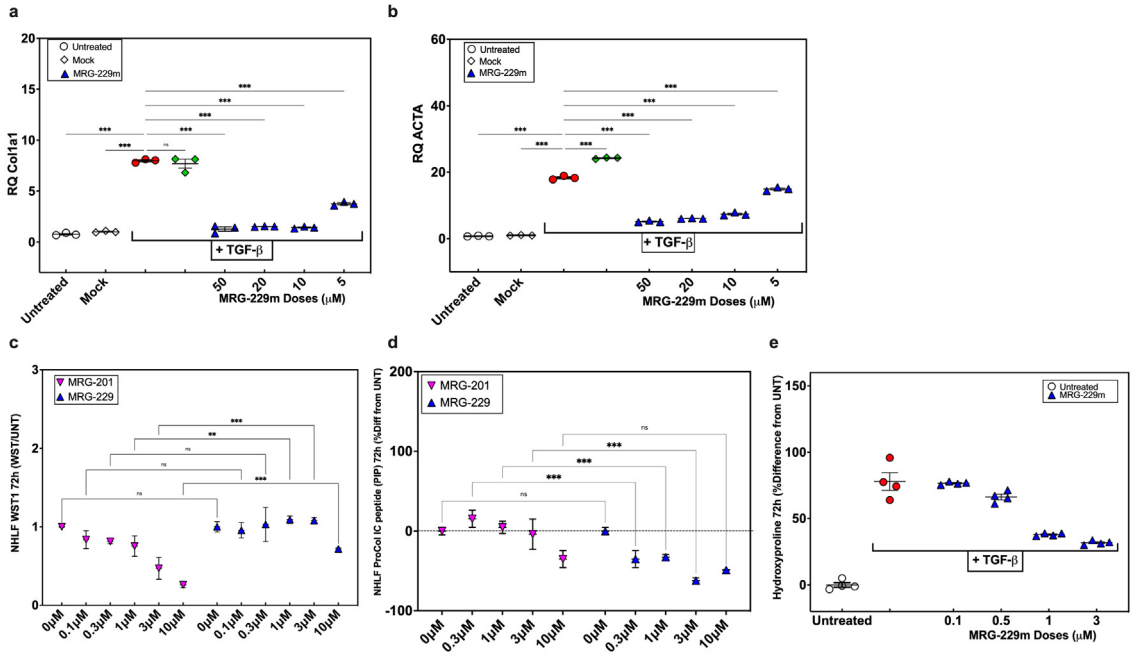

Figure 2. miR-29 reverses fibrosis in vitro. (a) RT-PCR of the miR-29b target gene *COL1A* in NHLFs. (b) RT-PCR of the miR-29b target gene *ACTA2* in NHLFs. (c) Cell viability in NHLFs treated with increasing concentrations of MRG-201 or MRG-229. (d) Reduction of procollagen I C-peptide secretion in NHLFs treated with increasing concentrations of MRG-201 or MRG-229. (e) Dose-dependent collagen secretion assessed by accumulation of hydroxyproline levels in LL29 cells at 72h treated with TGF-Beta to induce fibrosis and treated with increasing concentrations of MRG-229 as indicated. All experiments were performed on at least three biological replicates. Statistical analyses Ordinary one-way ANOVA (****P<0.001*) were performed in GraphPad Prism.

fibrosis mouse model: first, a prophylactic paradigm, in which we administered compound at day 3 following bleomycin administration and collected tissue at day 14 (Figure 4a). We compared MRG-229 to MRG-201 in the prophylactic setting. Given that MRG-201 requires a 100 mg/kg dosing to achieve efficacy, we assessed whether we could lower MRG-229 to a commercially viable dosage. Accordingly, three days after bleomycin administration, we intravenously injected MRG-201 (100 mg/kg) and MRG-229 (10 mg/kg) twice weekly. At day 14 we found a comparable down-regulation of miR-29 direct targets as well as non-direct targets (i.e., *CTGF*) in MRG-201 and MRG-229 bleomycin-injured lungs (Figure 4c). In contrast, an unconjugated version of MRG-229 showed no *in vivo* activity compared to bleomycin/saline controls (Figure 4d). Similarly, bleomycin-treated animals injected with 100 mg/kg MRG-201 or 10 mg/kg MRG-229 showed reductions in total collagen content compared to controls as assessed by trichome staining (Figure 4b). Overall, these dosing comparison experiments suggested that MRG-229 could be dosed at 10 mg/kg in mice to achieve a similar efficacy response as MRG-201 at 100 mg/kg.

We next asked if the anti-fibrotic effects observed with MRG-229 in mice extended to a therapeutic dosing paradigm (Figure 5a). Hence, we initiated twice-weekly dosing of 10 mg/kg MRG-229 10 days after bleomycin injury and collected tissue at day 21. In analysis of bronchoalveolar lavage fluid (BALF), we detected a ~20% reduction in IGF-1 levels, a known miR-29 target, and a ~40% reduction of TIMP1, a potential IPF biomarker in bleomycin-injured mice treated with MRG-229 relative to saline (Figure 5b). In quantitative histopathological analyses, we found that MRG-229 significantly reduced collagen deposition relative to saline, and preserved regions of normal alveoli architecture (Figure 5c, d).

Next, we asked whether subcutaneous administration of MRG-229 would achieve comparable *in vivo* efficacy to intravenous administration in the bleomycin-induced lung fibrosis model. Using regulation of profibrotic genes as our readout for varying doses of MRG-229 at 2, 5, 10, or 20 mg/kg administered either subcutaneously or intravenously in the prophylactic paradigm, we found that subcutaneous MRG-229 dosing achieves therapeutic efficacy between 2 and 5 mg/kg (Figure 5e). Next, we performed sandwich-based ELISA assay from lung tissue homogenate to compare distribution in the lung upon intravenous or subcutaneous administrations, we found that MRG-229 distribution was comparable and dose-proportionate between subcutaneously and intravenously routes (Figure 5f). These data support the potential for MRG-229 to be administered subcutaneously, while achieving therapeutic

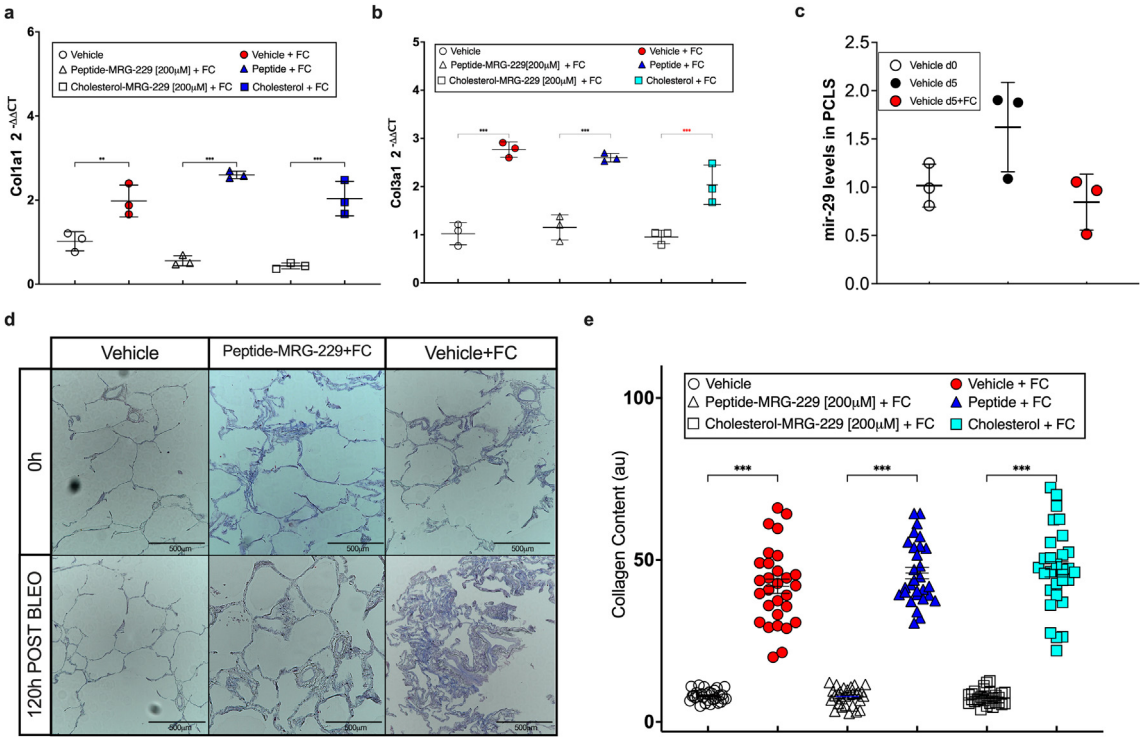

Figure 3. MRG-229 reverses fibrosis in a human Precision-Cut Lung Slice (hPCLS) model (blinded experiment). (a) RT-PCR analysis of *COL1A1* relative expression (b) RT-PCR analysis of *COL3A1* relative expression. (c) RT-PCR analysis of miR-29 level in human PCLS after 120 hrs in media + FC. (d) Masson Trichrome on human PCLS from healthy donors, cultured with either a fibrosis-inducing cocktail or vehicle for 120 hrs with daily media changes, treated with a peptide or a cholesterol-conjugated MRG-229 mimic. (e) Graph depicts quantification of collagen levels after 120 hrs on histology. Statistical analyses Ordinary one-way ANOVA (****P<0.001*) were performed in GraphPad Prism.

efficacy at a significantly lower and more commercially viable dosing regimen than MRG-201.

MRG-229 administration is associated with a favourable safety profile

Next, we assessed MRG-229 safety and toxicity profiles. From the dose-response and route of administration studies in mice (Figures 4 and 5), our initial assessment of liver enzyme function and kidney damage markers showed that MRG-229 administration was not associated with any detrimental effect on either organ (even in the presence of bleomycin) at up to 10 mg/kg biweekly dosing (Figure 6). Furthermore, we performed a 2-week repeat dose-range study of intravenous MRG-229 in Sprague Dawley Rats (Non-GLP) (Table 1). Rats received formulation buffer (10 mM phosphate buffer diluted with isotonic buffered saline) or MRG-229 at 3, 10 or 30 mg/kg on days 1, 4, 7, 11 and 14, after which we collected blood for hematology, coagulation, and serum chemistry analyses from the vena cava of fasted animals at necropsy on Day 15. Using metabolic cages, we also collected and analysed urine samples from fasted animals on Day 15. In addition, we performed gross pathology examinations and organ weight measurements on all animals at the terminal necropsy, and histopathology examination on all tissues from Groups 1 (vehicle treated) and 4 (30 mg/kg MRG-229 treated), including gross lesions, liver, kidneys, spleen, lungs, and heart, from Groups 2 (3 mg/kg MRG-229) and 3 (10 mg/kg MRG-229) animals. Overall, we observed no measurable differences in body weight, food consumption or clinical observations of vehicle- or MRG-229-treated rats. Similarly, we did not observe any differences in hematology, clinical chemistry, coagulation, or urinalysis parameters. In histopathology analyses, we found that MRG-229 treatment was associated with minimal basophilic granularity in the tubular epithelium of the kidney with minimal tubular vacuolation found in one animal. In summary, MRG-229 administered intravenously at 3, 10, and 30 mg/kg twice weekly for two weeks in rats was well tolerated in both males and females, with no observable adverse effects at any dose tested.

To assess potential toxicokinetic characteristics of MRG-229 by intravenous administration, we added three additional rats to Group 3 (10 mg/kg MRG-229) (Table 1). Samples for toxicokinetic analysis were

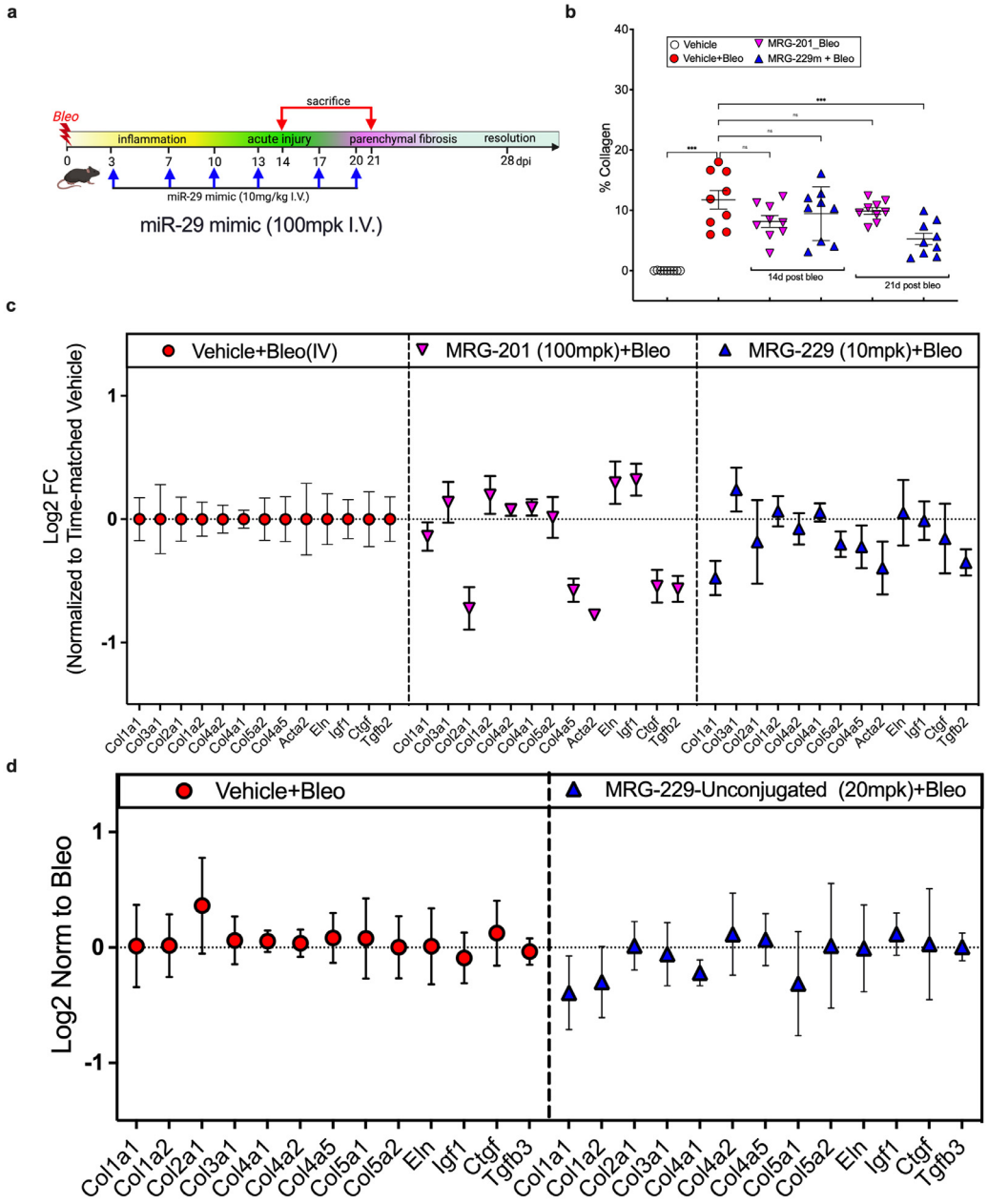

Figure 4. Day 14 analysis of prophylactic dosing of MRG-201 at 100 mpk and peptide-conjugated MRG-229 mimic at 10 mpk in the bleomycin-induced lung fibrosis model. (a) Schematic of prophylactic dosing paradigm. Bleomycin-treated mice were dosed through intravenous injection with saline, **MRG-201** on days 3, 7, 10 and 13. On day 14, animals were sacrificed, and lung tissue analysed. (b) Mean % total lung collagen quantified by Orbit machine learning image analysis software in bleomycin-induced mice treated with MRG-201 or MRG-229. (c) qPCR analysis of downregulated gene expression levels of a panel of fibrosis-associated genes in lung harvested from bleomycin-induced mice treated with either MRG-201 or MRG-229. C. (d) qPCR analysis of downregulated gene expression levels of a panel of fibrosis-associated genes in lung harvested from bleomycin-induced mice treated with either saline or the MRG-229-unconjugated with all the stability modifications but lacking the BiPPB conjugate. Statistical analyses Ordinary one-way ANOVA (****P<0.001*) were performed in GraphPad Prism. mpk - mg/Kg.

collected on study day 1 and 15 before dosing and at 5 min, 30 min, 1 hr, 2 hrs, 4 hrs, 8 hrs and 24 hrs after injection for Group 3. Groups 2 and 4 had toxicokinetic samples collected on study Day 1 and 14 before dosing and at 5 min after injection. Plasma concentrations of MRG-229 decreased rapidly following intravenous administration, with 5 out of 6 24 hr plasma samples testing below the limit of quantification (BLOQ) (Supp

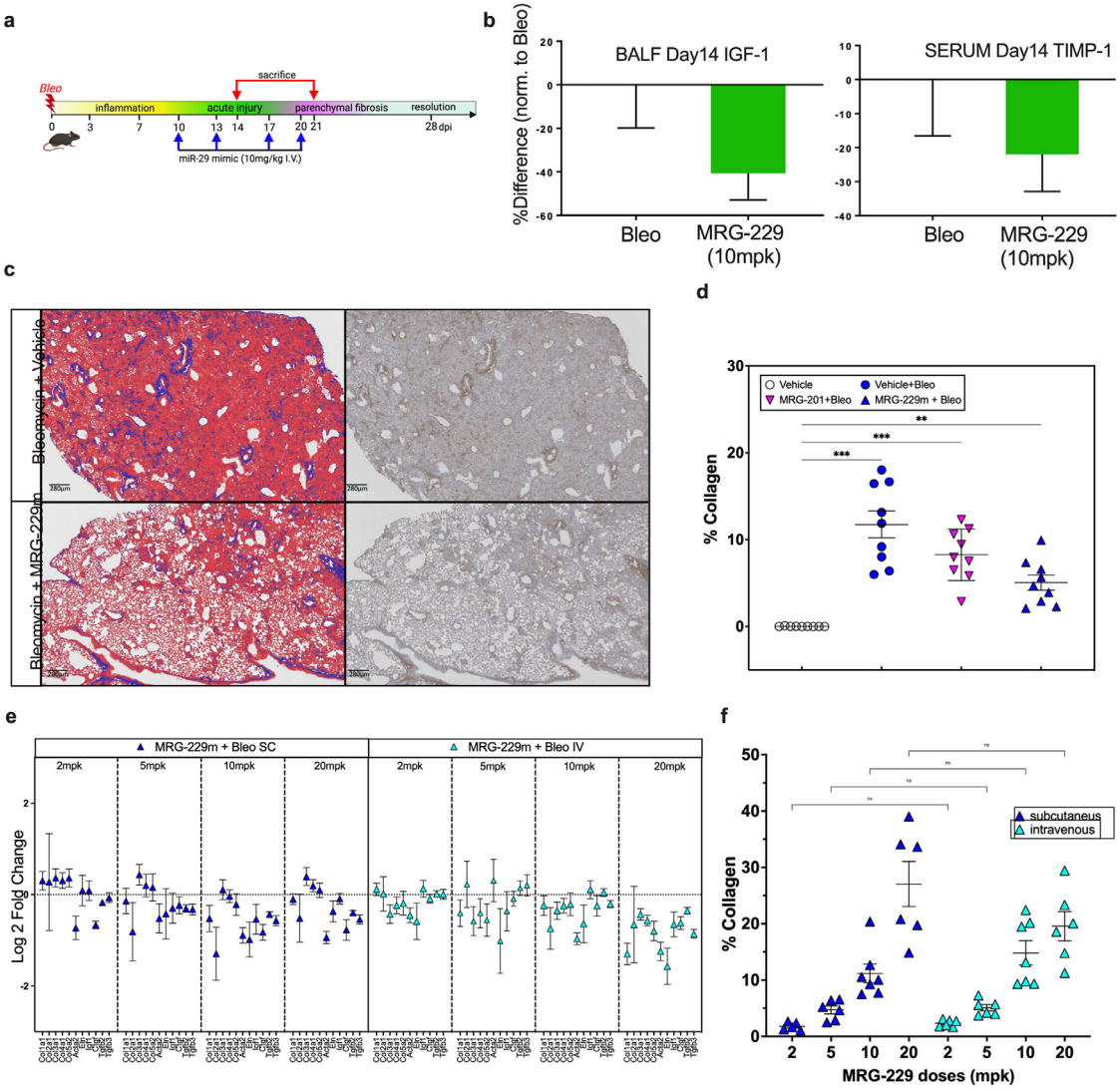

Figure 5. Day 21 analysis of therapeutic dosing of MRG-201 at 100 mpk and MRG-229 at 10 mpk in the bleomycin-induced lung fibrosis model (a) Schematic of therapeutic dosing paradigm. Bleomycin-treated mice were dosed through intravenous injection with saline, MRG-201 at 100 mpk, or MRG-229 at 10 mg/Kg, on days 10, 13, 17 and 20. On day 21, animals were sacrificed, and lung tissue analysed. (b) ELISA analysis of IGF-1 levels in bronchoalveolar lavage fluid (left) and TIMP-1 levels in serum (right) harvested from mice treated with either saline or MRG-229. (c) representative Masson Trichrome-stained histopathology images of saline-treated (top) and MRG-229-treated (bottom) lung sections. (d) mean % total lung collagen quantified by Orbit machine learning image analysis software in bleomycin-induced mice treated with MRG-201 or MRG-229. (e lung distribution of MRG-229 at different doses of either subcutaneous or intravenous injection. (f) lung distribution of MRG-229 at different doses of either subcutaneous or intravenous injection. Statistical analyses Ordinary one-way ANOVA (***P<0.001*) were performed in GraphPad Prism. mpk - mg/Kg

Table 1). Selected pharmacokinetic parameters for the TK animals were as expected (Supp Table 2). Last dose C_{max} values across the three dose levels were approximately dose proportional, with a trend towards sub proportional increases in C_{max} with increases in dose with no apparent gender differences observed (Suppl Table 3). Finally, to assess MRG-229 distribution to organ tissues, we collected samples from heart, liver, lung, kidney, and spleen tissues from animals in terminal Groups 2-4 (Supp Table 1). High concentrations of drug were detected in kidney, moderate in liver, small in spleen, heart, and lung (Supp Table 4).

Intravenous delivery of MRG-229 in non-human primates shows no adverse effects

Toxicological studies of potential therapeutic compounds in non-human primates are critical to assess

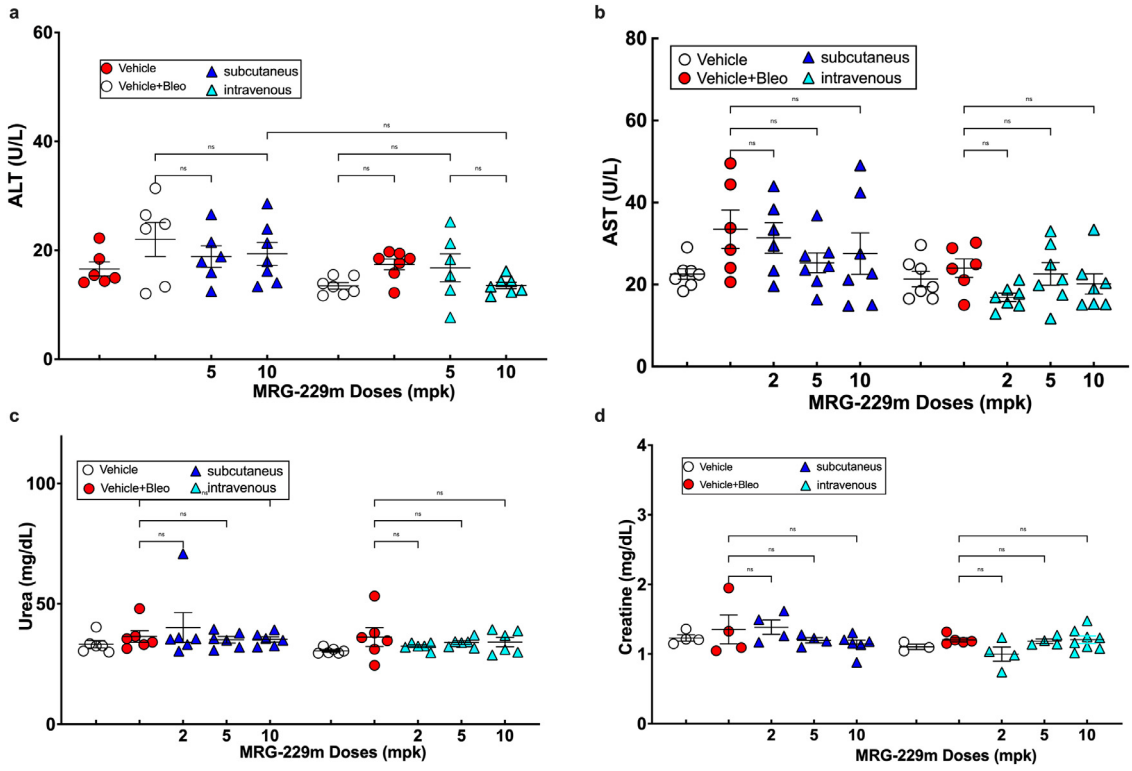

Figure 6. Liver ALT and AST (a, b), and Kidney Urea and Creatinine c, d), assessments following miR-29 administration. Assessment of liver function enzymes and markers of kidney damage from the dose response and route of administration study showed no detrimental effect on liver or kidney function by MRG-229, even in the presence of bleomycin, up to 10 mg/kg biweekly administered. Statistical analyses Ordinary one-way ANOVA (****P<0.001*) were performed in GraphPad Prism. mpk - mg/Kg

their potential for translation to the clinic. To this end, we assessed MRG-229 in a dose range finding study in non-human primates (NHPs) (Table 2). We administered MRG-229 by intravenous injection to naïve cynomolgus monkeys (1 animal/sex/group) at concentrations of 0, 5, 15, and 45 mg/kg on days 1, 4, 7, 11, 15, and performed necropsy and sample collection on day 16 (Supp Table 5). We did not observe any notable parameters related to clinical observations, food consumption, or bodyweights (data not showed). We found no evidence of MRG-229 related findings in the hematology, clinical chemistry, coagulation, or urinalysis parameters assessment. In all dose groups, a slight decrease in hematocrit and an increase in reticulocytes on day 2 and day 16 relative from pre-treatment values, likely due to the extensive blood sampling protocol requirements. We did not identify any MRG-229-related histologic findings in tissues from Group 4 (45 mg/kg MRG-229), suggesting that the dose tested was well tolerated.

Group	Test or Control Articles	Dose Level (mg/kg)	Number of Animals Males/Females
1	Control	0	1/1
2	MRG-229	5	1/1
3	MRG-229	15	1/1
4	MRG-229	45	1/1

***Table 1*: Study design for 2-week repeat dose study of MRG-229 by intravenous administration in Sprague Dawley Rats (Non-GLP).**

MRG-229 plasma concentrations in treated monkeys decreased rapidly (by 24 h MRG-229 concentration decreased to > 0.5% of initial values, with several samples testing below the quantifiable level (BQL) (Suppl Table 6). Mean and individual pharmacokinetic parameters are reported in Suppl Table 7. Male and female showed similar PK results in all groups. As expected for intravenous bolus, T_{max} was at the time of the first sample collected after dosing (5 min) for almost all animals. C_{max} concentrations were expectedly high following the intravenous bolus dose, reaching day 1 mean values of 312 µg/mL for the MRG-229 45 mg/kg group. There was no accumulation observed for either C_{max} or AUC last values from Day 1 to 15 weeks to cynomolgus monkeys (Supp Table 7), however C_{max} and AUC_{last} values across the MRG-229 dose groups were nearly perfectly proportional, with dose normalized values being very similar across dose group for both day 1 and day 15 PK

Group	Route of Administration	Test or Control Articles	Dose Level (mg/kg)	Terminal Animals (M/F)
1	IV Injection	Control	0	3/3
2		MRG-229	3	3/3
3			10	3/3
4			30	3/3

***Table 2*: Toxicological study design of MRG-229 in non-human primates.**

curves (Suppl Table 7), and nearly perfectly linear increases in C_{max} and AUC_{last} values across the dose range were observed (Suppl Table 8). Finally, 24 hours after the final dose, MRG-229 was detected in the lung tissue, consistent with our earlier mouse data (Supp Table 3).

Exosomal miR-29b levels in plasma and serum are associated with mortality in two cohorts of IPF patients

miR-29 is a known regulator of fibrosis and a decrease in its expression is associated with lung fibrosis.[11,30,31] We reasoned that miR-29 levels in humans could be used to develop a precision medicine-based approach to identify individuals at risk of death. To potentially identify such patients, we examined circulating and exosomal miR-29b levels in a cohort of 46 and 213 patients with IPF diagnosis recruited from Yale and Nottingham Universities Profile Cohort), respectively. Table 3 shows the clinical characteristics of IPF patients in both cohorts. For each patient, we performed miRNA extraction from plasma or serum samples isolated from blood, followed by multiplexed, color-coded probe pairs to assess levels of miR-29b specifically. miRNA data was normalized using top 100 normalization and log2 transformed miR-29b levels were used for statistical analysis. Receiving Operating characteristics (ROC) curves were used to determine the optimal threshold for mortality association using exosomal miR-29b in IPF patients from both Yale and Profile cohorts. Cox proportional hazard's models and Kaplan-Meir curves were used to determine the association between exosomal miR-29b levels, adjusted to GAP index, and IPF mortality.

	Yale cohort (N=46)	Profile cohort (N=213)
Age (± SD)	68.5 (± 7.5)	73 (± 6.62)
Gender		
Male (%)	39	166
Female (%)	7	47
FVC% (± SD)	75.77 (± 9)	80.26 (± 22.15)
DLCO% (± SD)	49.1 (± 9.6)	41.7 (± 21.5)
GAP index (± SD)	3.96 (± 1.41)	2.56 (± 0.52)

***Table 3*: Clinical profile characteristics of IPF patients in both cohorts.**

We found that ROC identified similar miR-29b exosomal RNA thresholds for mortality association in the Yale (plasma level threshold of 4.84) and Profile (serum level threshold of 4.32) cohorts. After adjusting for the GAP severity index, exosomal miR-29b levels in plasma (≤ 4.86) and serum (≤ 4.32) were significantly associated with mortality in the Yale (HR:0.156, 95%CI: 0.0404-0.6066, Statistical analyses Ordinary one-way ANOVA P=0.0073) and Profile (HR:0.5066, 95%CI: 0.2984-0.8599, Statistical analyses Ordinary one-way ANOVA P=0.011) cohorts, respectively (Figures 7A, B).

Discussion

In this study, we report the development of MRG-229, a next-generation miR-29 mimic capable of reversing fibrosis-associated molecular transcription and secretion phenotypes in human cellular lung fibrosis models. Relative to our first-generation compound MRG-201, MRG-229 achieved comparable levels of fibrosis reversal *in vitro* at a ten-fold lower systemic dose level, an improvement which enabled us to explore both efficacy and safety parameters using commercially viable doses in preclinical animal models. In bleomycin-induced mice, we found that MRG-229 effectively achieved downregulation of direct and indirect miR-29 profibrotic target genes concomitant with reduced collagen secretion and preserved lung alveolar architecture. We also found that MRG-229 administration was associated with a favourable safety profile at 10 mg/kg dosing in mice, at 30 mg/kg in rats and at 45 mg/kg in NHP. Intravenous administration is inconvenient to patients and associated with a higher risk for adverse events relative to oral and subcutaneous delivery routes. In bleomycin-induced mice, we assessed both intravenous and subcutaneous MRG-229 administration and found that both delivery approaches reduced pro-fibrotic gene expression programs at therapeutically relevant doses. We further demonstrated that low levels of miR-29 in serum or plasma may be associated with increased mortality in IPF patients and could potentially be used to identify patients that could have a survival benefit from MRG-229 administration. Taken together, these data suggest that administration of MRG-229 is safe and effective at commercially viable dosing levels and may be an attractive candidate for treatment of IPF.

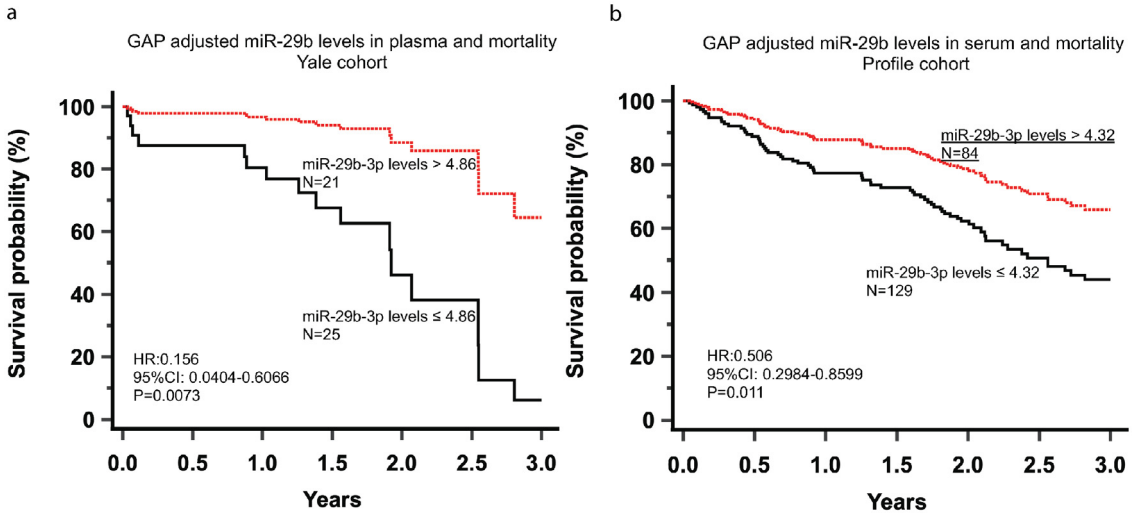

Figure 7. miR-29 survival in 2 IPF cohort: ROC identified similar miR-29b exosomal RNA thresholds for mortality prediction in the Yale (plasma level threshold of 4.84) and Profile (serum level threshold of 4.32) cohorts. After adjusting for the GAP severity index, exosomal miR-29b levels in plasma ($\leq$ 4.86) and serum ($\leq$ 4.32) were significantly associated with mortality in the Yale (HR:0.156, 95%CI: 0.0404-0.6066, Statistical analyses Ordinary one-way ANOVA P=0.0073) and Profile (HR:0.5066, 95%CI: 0.2984-0.8599, Statistical analyses Ordinary one-way ANOVA P=0.011) cohorts, respectively. Figures 7a and 7b.

A recent study reported the results of a Phase 1 clinical trial in which healthy volunteers (n=47) were treated with intradermal miR29b mimetic MRG-201 or placebo injections after receiving skin incisions. In this trial, MRG-201 had no impact on normal wound healing but significantly decreased fibroplasia relative to placebo. This study serves as a proof of concept for local MRG-201 administration in human skin as an approach to prevent formation of a fibrotic scar.[17] In the context of our paper, this is an important result as it demonstrates that the miR-29b mimetic has a potential antifibrotic effect *in vivo* in humans. Indeed, in our study we show that MRG-229 can partially reverse fibrosis in human PCLS treated with a profibrotic cocktail. Our PCLS results establish a strong case that miR-29 mimicry will be a potential antifibrotic in humans, and that MRG-229, given its safety profile, stability and superior pharmacodynamic properties, may be a suitable agent to confer this effect. Of note, levels of MRG-229 were detected not only in the lung but also in several other organs. Such systemic delivery is an important limitation of oligo-based therapeutics in general; however previous studies have demonstrated that there is minimal on-target activity or pharmacodynamics in tissues where the miRNA is not dysregulated. Longer toxicology studies will need to be performed prior to more chronic dosing in humans, and while PK studies in rats and NHP provide important guidance on dosing and frequency of administration, dose escalation and PK studies in humans will be required to make final determinations before clinical efficacy trials. Finally, although in this manuscript we focus on systemic administration, inhaled delivery may still be considered as an alternative mode of administration to increase targeting of MRG-229 specifically to the lung.

A common challenge with IPF therapeutics is that there is little evidence that the target mechanism is in fact implicated in the patients we treat. In the case miR-29, the therapeutic premise is straightforward: expression of miR-29 is decreased in lung fibrosis[11,30,31] (as it is in nearly every fibrotic condition), leading to aberrant expression of profibrotic genes controlled by miR-29b, which is restored by delivery of the miR-29b mimetic MRG-229. McDonough et al assessed gene expression changes in the differentially affected regions in the IPF lung,[31] and demonstrated that miR-29 was decreased in the IPF lung even in relatively conserved areas, whereas genes known to be regulated by miR-29 were increased as fibrosis progressed. Unfortunately, it is impossible to assess miR-29 in the lung in most patients as biopsies are limited. In this manuscript, we provide an observation that may be very important in this context. We demonstrate that in two independent cohorts, decreased peripheral blood exosomal miR-29 is associated with worse prognosis in patients with IPF. This finding suggests a connection between reduced miR-29 levels and IPF progression and could potentially be used in the future as a companion diagnostic. A limitation from this analysis is the fact that the cohorts we studied had differences in starting material (plasma – Yale cohort and serum – Profile cohort), sample size and disease severity. These differences may have affected our ability to identify similar miR-29 cut offs for mortality association. Future studies should be performed to validate our

findings in multiple, large, and similar cohorts of patients using the same starting material (plasma or serum) to develop a prediction model that can be easily replicated in other cohorts. Nonetheless, the fact that low blood plasma and serum levels of miR29-b are associated with mortality in IPF patients supports the use of miR-229 as a potential therapy. Taken together, the findings reported here represent a solid range of IND-enabling work for further clinical development of MRG-229 in pulmonary fibrosis indications.

Contributors

NK, RLM, MC, GY, SR, KR, and LP conceived, designed, and analysed experiments and results. BD, GJ, SI, GS, SJ, RB collect and analysed samples for the Profile Cohort. MC, KR, RN, GY, NA, DS, FA, MS, GD, ~~OD~~ and JHM performed and analysed results. MC, RLM and NK wrote the manuscript. All authors read and approved the final version of the manuscript. RLM and NK have verified the underlying data.

Data sharing statement

All data are available in the main text or the supplementary materials.

Declaration of interests

All miRagen employees were employed by miRagen Therapeutics, Inc at the time of studies and may have held stock in the company at the time. NK served as a consultant to Boehringer Ingelheim, Third Rock, Pliant, Samumed, NuMedii, Theravance, LifeMax, Three Lake Partners, Optikira, Astra Zeneca, RohBar, Veracyte, Augmanity, CSL Behring, Galapagos, Arrowhead, Spinnova, and Thyron over the last 3 years, reports Equity in Pliant and Thyron, and a grant from Veracyte, Boehringer Ingelheim, BMS and non-financial support from MiRagen and Astra Zeneca. NK has IP on novel biomarkers and therapeutics in IPF licensed to Biotech. GJ has institutional support for PROFILE study through an MRC Industrial Collaboration Agreement (MICA) (GSK). GJ has grants or contracts from Astra Zeneca, Biogen, Galecto, GSK, Nordic Biosciences, RedX, Pliant, with all payments going to his institutions. GJ served as consultant to Bristol Myers Squibb, Chiesi, Daewoong, Veracyte, Resolution Therapeutics, Pliant. GJ had payment or honoraria for lectures, presentations, speaker bureaus, manuscript writing or educational events to Boehringer Ingelheim, Chiesi, Roche, PatientMPower, AstraZeneca. GJ has participation on a data safety monitoring board or advisory board to Boehringer Ingelheim, Galapagos, Vicore. GJ has leadership or fiduciary role in other board, society, committee, or advocacy group, paid or unpaid to NuMedii. GJ is also a trustee to Action for Pulmonary Fibroisis. SR was provided funds for travelling to conferences by miRagen Therapeutics. SR has a patents planned, issued or pending: US Patent Application 20200318113 (miRagen Therapeutics). SR owns Miragen stock at the time this work was performed.

Acknowledgements

This work was supported by NIH NHLBI grants UH3HL123886, R01HL127349, R01HL141852, U01HL145567.

Supplementary materials

Supplementary material associated with this article can be found in the online version at doi:10.1016/j.ebiom.2022.104304.

References

1 Roberts TC, Langer R, Wood MJA. Advances in oligonucleotide drug delivery. *Nat Rev Drug Discov*. 2020;19:673–694.
2 Martinez F J, Collard H R, Pardo A, et al. Idiopathic pulmonary fibrosis. *Nat Rev Dis Primers*. 2017;3:1–19.
3 Finkel R S, Chiriboga C A, Vajsar J, et al. Treatment of infantile-onset spinal muscular atrophy with nusinersen: a phase 2, open-label, dose-escalation study. *Lancet*. 2016;388(10063):3017–3026.
4 Adams D, Gonzalez-Duarte A, O'Riordan W D, et al. Patisiran, an RNAi therapeutic, for hereditary transthyretin amyloidosis. *N Engl J Med*. 2018;379:11–21.
5 Zhou J, Xu Q, Zhang Q, Wang Z, Guan S. A novel molecular mechanism of microRNA-21 inducing pulmonary fibrosis and human pulmonary fibroblast extracellular matrix through transforming growth factor β1—mediated SMADs activation. *J Cell Biochem*. 2018;119:7834–7843.
6 Zhang S, Liu H, Liu Y, et al. miR-30a as potential therapeutics by targeting tet1 through regulation of Drp-1 promoter hydroxymethylation in idiopathic pulmonary fibrosis. *Int J Mol Sci*. 2017;18(3):1–12.
7 Li P, Zhao G, Chen T, et al. Serum miR-21 and miR-155 expression in idiopathic pulmonary fibrosis. *J Asthma*. 2013;50(9):960–964.
8 Tsitoura E, Wells A U, Karagiannis K, et al. MiR-185 /AKT and miR-29a / collagen 1a pathways are activated in IPF BAL cells. *7, Oncotarget*. 2016;7(46):74569–74581.
9 Bibaki E, Tsitoura E, Vasarmidi E, et al. MiR-185 and miR-29a are similarly expressed in the bronchoalveolar lavage cells in IPF and lung cancer but common targets DNMT1 and COL1A1 show disease specific patterns. *Mol Med Rep*. 2018;17(5):7105–7112.
10 Huang C, Xiao X, Yang Y, et al. MicroRNA-101 attenuates pulmonary fibrosis by inhibiting fibroblast proliferation and activation. *J Biol Chem*. 2017;292(40):16420–16439.
11 Cushing L, Kuang P P, Qian J, et al. miR-29 is a major regulator of genes associated with pulmonary fibrosis. *Am J Respir Cell Mol Biol*. 2011;45(2):287–294.
12 Cushing L, Kuang P, Lü J. The role of miR-29 in pulmonary fibrosis. *Biochem Cell Biol*. 2015;93(2):109–118.
13 Wang B, Komers R, Carew R, et al. Suppression of microRNA-29 expression by TGF-β1 promotes collagen expression and renal fibrosis. *J Am Soc Nephrol*. 2012;23(2):252–265.
14 Pandit KV, Milosevic J, Kaminski N. MicroRNAs in idiopathic pulmonary fibrosis. *Transl Res*. 2011;157(4):191–199.
15 Montgomery R L, Yu G, Latimer P A, et al. Micro RNA mimicry blocks pulmonary fibrosis. *EMBO Mol Med*. 2014;6(10):1347–1356.
16 Van Rooij E, Sutherland L B, Thatcher J E, et al. Dysregulation of microRNAs after myocardial infarction reveals a role of miR-29 in cardiac fibrosis. *Proc Natl Acad Sci USA*. 2008;105(35):13027–13032.
17 Gallant-Behm CL, Piper J, Lynch J M, et al. A microRNA-29 mimic (Remlarsen) represses extracellular matrix expression and fibroplasia in the skin. *J Invest Dermatol*. 2019;139(5):1073–1081.

18 Nogimori T, Furutachi K, Ogami K, et al. A novel method for stabilizing microRNA mimics. *Biochem Biophys Res Commun*. 2019;511 (2):422–426.
19 Tsui N B Y, Ng E K O, Lo Y M D. Stability of endogenous and added RNA in blood specimens, serum, and plasma. *Clin Chem*. 2002;48(10):1647–1653.
20 Gaus H J, Gupta R, Chappell A E, et al. Characterization of the interactions of chemically-modified therapeutic nucleic acids with plasma proteins using a fluorescence polarization assay. *Nucleic Acids Res*. 2019;47(3):1110–1122.
21 Hammond S M, Aartsma-Rus A, Alves S, et al. Delivery of oligonucleotide-based therapeutics: challenges and opportunities. *EMBO Mol Med*. 2021;13(4):1–23.
22 Raghu G, Collard H R, Egan J J, et al. An official ATS/ERS/JRS/ALAT statement: idiopathic pulmonary fibrosis: evidence-based guidelines for diagnosis and management. *Am J Respir Crit Care Med*. 2011;183(6):788–824.
23 Lederer DJ, Martinez FJ. Idiopathic pulmonary fibrosis. *N Engl J Med*. 2018;378(19):1811–1823.
24 Huang Y H, Yang Y L, Wang F S. The role of miR-29a in the regulation, function, and signaling of liver fibrosis. *Int J Mol Sci*. 2018;19(7):1–8.
25 Alsafadi HN, Staab-Weijnitz C A, Lehmann M, et al. An ex vivo model to induce early fibrosis-like changes in human precision-cut lung slices. *Am J Physiol Cell Mol Physiol*. 2017;312(6):896–902. https://doi.org/10.1152/ajplung.00084.2017.
26 Chen Y, Yu Q, Xu CB. A convenient method for quantifying collagen fibers in atherosclerotic lesions by imagej software. *Int J Clin Exp Med*. 2017;10(10):14904–14910.
27 Bansal R, Prakash J, De Ruiter M, et al. Interferon gamma peptidomimetic targeted to hepatic stellate cells ameliorates acute and chronic liver fibrosis in vivo. *J Control Release*. 2014;179:18–24.
28 Neuhaus V, Schaudien D, Golovina T, et al. Assessment of long-term cultivated human precision-cut lung slices as an ex vivo system for evaluation of chronic cytotoxicity and functionality. *J Occup Med Toxicol*. 2017;12:1–8. https://doi.org/10.1186/s12995-017-0158-5.
29 Liu G, Betts C, Cunoosamy D M, et al. Use of precision cut lung slices as a translational model for the study of lung biology. *Respir Res*. 2019;20(162):1–14.
30 Riedel L, Fischer B, Ly T, et al. microRNA-29b mediates fibrotic induction of human xylosyltransferase-I in human dermal fibroblasts via the Sp1 pathway. *Sci Rep*. 2018;8:1–14.
31 McDonough JE, Ahangari F, Li Q, et al. Transcriptional regulatory model of fibrosis progression in the human lung. *JCI Insight*. 2019;4(22):1–15.